Counterion Effects on Hexadecyltrimethylammonium Surfactant Adsorption and Self-Assembly on Silica

Stephanie B. Velegol,[†] Barry D. Fleming,[‡] Simon Biggs,[‡] Erica J. Wanless,[‡] and Robert D. Tilton*,[†]

Department of Chemical Engineering, Colloids Polymers and Surfaces Program, Carnegie Mellon University, Pittsburgh, Pennsylvania 15213, and Department of Chemistry, University of Newcastle, Callaghan, NSW 2308, Australia

Received August 13, 1999. In Final Form: November 18, 1999

Combining optical reflectometry and atomic force microscopy (AFM), we have studied the effects of the surfactant counterion on the adsorption isotherms, kinetics, and layer structure for cationic hexadecyltrimethylammonium ($C_{16}TA^+$) surfactants on negatively charged silica surfaces. The adsorption kinetics suggest that the adsorption mechanism changes at the critical micelle concentration (cmc). A change in mechanism is also suggested by differences observed in the state of interfacial self-assembly on either side of the cmc. Above the cmc, increasing the binding affinity of the counterion (from chloride to bromide) increased the surface excess concentration by approximately 60% and changed the structure of the adsorbed surfactant layer from aggregates with circular projections to wormlike micelles. The addition of 10 mM KCl or KBr increased the surfactant surface excess concentration for both counterions. Below the cmc, the counterion has only a small effect on the structure of the adsorbed layer, and the isotherms are similar, provided the surfactant concentration is scaled by the appropriate cmc. By quantitatively analyzing the AFM images and comparing this to the surface excess concentration measured by reflectometry, we determined that surfactants pack differently in adsorbed aggregates than they do in aggregates formed by self-assembly in solution. Finally, we show that an impurity present in poly(vinyl chloride) tubing explains anomalous adsorption behavior previously reported for $C_{16}TAB$ on silica.

Introduction

Surfactant adsorption to solid/aqueous interfaces is important in many processes, including suspension stabilization, mineral flotation, detergency, wetting, and fluid penetration into porous substrates. There has been much work on the equilibrium adsorption of cationic quaternary ammonium surfactants to anionic surfaces and the following mechanism has emerged, primarily from the shape of the adsorption isotherms: adsorption occurs initially via attractive electrostatic interactions between the cationic headgroup and the anionic surface. Once the extent of adsorption is sufficient to neutralize the surface charge, adsorption continues cooperatively via interactions between the hydrophobic tails, leading to surfactant self-assembly on the surface at higher coverages.[1] Recent advances in optical, spectroscopic, and microscopic techniques have made it possible to study this interfacial self-assembly process in greater detail.

Counterions are recognized to play a critical role in the adsorption mechanism[2] yet the origins of the counterion effects are not clear. In solution, counterions stabilize ionic surfactant micelles by binding to the micelle surface and screening the electrostatic repulsions between the ionic headgroups. In this way, the counterion binding affinity influences the bulk self-assembly process. For example, Bartet et al.[3] report that bromide ions have a 5-fold greater binding affinity for cationic hexadecyltrimethylammonium ($C_{16}TA^+$) surfactant micelles than have chloride ions, based on their ion exchange constants relative to hydroxyl ions. The greater binding affinity of Br^- to $C_{16}TA^+$ is also evident in the degree of micellar counterion binding: 71% for bromide ($C_{16}TAB$) vs 55% for chloride ($C_{16}TAC$).[4] Accordingly, the cmc of $C_{16}TAB$ is lower than the cmc of $C_{16}TAC$ (0.94 mM vs 1.4 mM in deionized water). Counterions also affect the micelle sphere to rod transition in solution. $C_{16}TAB$ forms rodlike micelles at 80 mM KBr while $C_{16}TAC$ micelles remain spherical until 1200 mM KCl.[5] There is also some evidence that bromide penetrates more deeply into the surface of the micelle, and this aids in stabilizing the sphere to rod transition in solution.[5]

Uncertainty about the structure of adsorbed surfactant layers has complicated experimental efforts to quantify the role of counterions in surfactant adsorption. This is further compounded by the inability of most techniques to specifically detect adsorbed counterions in situ. There have been some attempts to determine the degree of counterion binding to adsorbed quaternary ammonium surfactants. For example, Chen et al. studied the adsorption of $C_{16}TA^+$ to mica with various counterions using X-ray photoelectron spectroscopy on dried films. They also used the surface forces apparatus and a chloride-specific electrode for in situ studies. They found that both the final equilibrium state and the dynamics of surfactant adsorption depend on the presence of the counterions at the surface.[2] Pashley et al.[6] used the surface forces apparatus to measure forces between adsorbed layers of $C_{16}TAB$ on mica. Using the Poisson−Boltzmann equation and assuming bilayer adsorption, they estimated that 78% of adsorbed surfactants had bound counterions. This value

* Corresponding author. E-mail: tilton@andrew.cmu.edu. Tel: (412)-268-1159. Fax: (412)-268-7139.

[†] Carnegie Mellon University.

[‡] University of Newcastle.

(1) Somasundaran, P.; Fuerstenau, D. W. *J. Phys. Chem.* **1966**, *70*, 90.

(2) Chen, Y. L.; Chen, S.; Frank, C.; Israelachvili, J. *J. Colloid Interface Sci.* **1992**, *153*, 244.

(3) Bartet, D.; Gamboa, C.; Sepulveda, L. *J. Phys. Chem.* **1980**, *84*, 272−5.

(4) Lindman, B.; Puyal, M. C.; Kamenka, N.; Rymden, R.; Stilbs, P. *J. Phys. Chem.* **1984**, *88*, 5048−57.

(5) Magid, L. J.; Han, Z.; Warr, G. G.; Cassidy, M. A.; Butler, P. D.; Hamilton, W. A. *J. Phys. Chem. B* **1997**, *101*, 7919−7927.

(6) Pashley, R. M.; McGuiggan, P. M.; Horn, R. G.; Ninham, B. W. *J. Colloid Interface Sci.* **1988**, *126*, 569.

10.1021/la9910935 CCC: $19.00
Published on Web 01/12/2000

is similar to the degree of counterion binding to C_{16}TAB micelles in solution mentioned above. However, if the adsorbed layer actually consisted of curved aggregates rather than a homogeneous bilayer as later studies have indicated, a more complex distribution of charge at the interface would need to be considered in the Poisson−Boltzmann calculations.

More recently, there have been several studies using atomic force microscopy (AFM) to image the structure of adsorbed quaternary ammonium surfactant layers on hydrophilic substrates. Most of this work has used "soft contact" AFM where the tip is maintained at a finite separation from the adsorbed layer by repulsive electrostatic interactions.[7] Mica has traditionally been used as the model hydrophilic substrate because atomically smooth and clean surfaces are prepared easily. The majority of the AFM work has been done above the critical micelle concentration. For example, Ducker et al.[8,9] found that C_{16}TAB formed rods at 1.8 mM (twice the cmc in pure water) on mica with or without KBr (0−101 mM). Without KBr, rods initially formed on the surface but transformed into uniform sheets after 17−25 h.[9] The rods were stabilized by 10 mM KBr and became shorter and less linear with the addition of higher salt concentrations. More recently Patrick et al.[10] found that the chain length and headgroup size affected the structure of the adsorbed surfactant layer on mica. These effects on aggregate curvature followed the same trends found in solution.

Two recent studies have addressed, specifically, the role of counterions on the structure of adsorbed quaternary ammonium surfactant layers on mica. Lamont and Ducker[8] found that changing the counterion from Br^- to Cl^- led to a higher curvature of the absorbed surfactant structures at constant CTA^+ and alkali cation concentrations. However, with no salt present both C_{16}TAB and C_{16}TAC formed rods that transformed into flat bilayers over time. Patrick et al.[10] found that $C_{12}TA^+$ formed rods with Br^- and spheres with Cl^- in the absence of salt, while both C_{14}TAB and C_{14}TAC formed rodlike micelles.

Though mica is an excellent model surface for AFM studies, there is little supporting information in the literature on either the adsorbed amount or kinetics of adsorption, both of which are critical to understanding the adsorption process as a whole. Two similar anionic surfaces that have been widely studied with respect to cationic surfactant adsorption are silica and quartz. Rennie et al. used neutron reflectivity to study the adsorption of C_{16}TAB on crystalline quartz and postulated that either a defective bilayer or a layer of flattened micelles forms above the cmc.[11] Using optical reflectometry, we have previously reported both the adsorbed amount and kinetics of adsorption for C_{16}TAB on silica with and without 10 mM KBr.[12,13] The kinetic results in these publications suggested a change in the adsorption mechanism at the cmc. Eskilsson and Yaminsky also measured the adsorption of C_{16}TAB on silica using ellipsometry[14] and found that the equilibrium adsorbed amount increases from almost no adsorption at 5% of the cmc to an adsorption plateau value of 40 Å^2/molecule above the cmc.[14] Although it is tempting to compare results from silica or quartz to those found on mica, there are major differences that complicate the comparison. Mica has one ionizable site per 0.48 nm^2 as a result of isomorphous substitution of Al for Si in the crystal lattice.[15] The silica surface charge arises from dissociation of silanol residues. The charge density of silica depends on its acid/base treatment history, but a charge density of one per 20 nm^2 is representative near neutral pH.[16] Furthermore, mica is atomically smooth and crystalline, while silica is not.

There have been few AFM studies on silica. Manne and Gaub[17] found that C_{14}TAB formed spherical micelles on the silica surface at 2 × cmc. More recently, Liu and Ducker reported spherical micelles of C_{16}TAB on silica at 2 × cmc.[18] Subramanian and Ducker are also investigating the influence of counterions on shape transitions for alkyltrimethylammonium surfactants adsorbed on silica.[19]

In the effort to understand adsorption mechanisms, it is important to relate the adsorbed layer structure to the surface excess concentration. In this work we use optical reflectometry to measure surface excess concentrations and kinetics while using AFM to independently image adsorbed layers on identically prepared silica surfaces. We will show that the combination of the two techniques can provide new insight into the adsorption mechanism. We specifically compare the effects of bromide and chloride counterions on $C_{16}TA^+$ adsorption. We find that decreasing the binding affinity of the counterion (changing from Br^- to Cl^-) decreases the surface excess concentration and increases the curvature of the adsorbed aggregates at 10 × cmc. Above the cmc, the addition of a simple 1:1 electrolyte at 10 mM concentration increases the adsorbed amount in both cases. Below the cmc, the counterion has a small effect on the structure of the adsorbed layer and the isotherms are similar, provided the concentration is scaled by the appropriate cmc. When compared with mica under similar conditions, the structures we observe on silica have higher curvatures. Finally we discuss the origin of an anomalous pattern in C_{16}TAB adsorption isotherms we had reported previously.[12,13]

Experimental Section

We purified all water by reverse osmosis and subsequent passage through a MilliQ Plus (Millipore) system of ion exchange and activated carbon cartridges. For the reflectometry experiments, we obtained C_{16}TAB (>99% pure) from Sigma and C_{16}TAC (98% pure) from Fluka and further purified them by repeatedly washing with acetone. We obtained potassium bromide and potassium chloride (ACS grade) from Fisher Scientific and EM Science, respectively. For the AFM experiments, we used C_{16}TAB (>99% pure) and C_{16}TAC (>98% pure) from Fluka. We purchased the KBr from Ajax Chemicals and the KCl from Jaeger Chemicals. Both salts were AR grade and were roasted at 600 °C overnight before use. We prepared silica surfaces by thermal oxidation of optical grade silicon wafers (Lattice Materials) at 1000 °C for 10 min. This produced approximately 20 nm thick oxide layers atop the silicon wafers. We cleaned these surfaces by the procedure described in Pagac et al.[13] and Furst et al.[12] This left the surfaces perfectly wetted by water. Atomic force microscopy confirmed that these surfaces were free of particulate and/or organic contamination. We measured the RMS roughness

(7) Manne, S.; Cleveland, J. P.; Gaub, H. E.; Stucky, G. D.; Hansma, P. K. *Langmuir* **1994**, *10*, 4409−13.
(8) Lamont, R. E.; Ducker, W. A. *J. Am. Chem. Soc.* **1998**, *120*, 7602−7607.
(9) Ducker, W. A.; Wanless, E. J. *Langmuir* **1999**, *15*, 160−168.
(10) Patrick, H. N.; Warr, G. G.; Manne, S.; Aksay, I. A. *Langmuir* **1999**, *15*, 1685−1692.
(11) Rennie, A. R.; Lee, E. M.; Simister, E. A.; Thomas, R. K. *Langmuir* **1990**, *6*, 1031−4.
(12) Furst, E. M.; Pagac, E. S.; Tilton, R. D. *Ind. Eng. Chem. Res.* **1996**, *35*, 1566−74.
(13) Pagac, E. S.; Prieve, D. C.; Tilton, R. D. *Langmuir* **1998**, *14*, 2333−2342.
(14) Eskilsson, K.; Yaminsky, V. V. *Langmuir* **1998**, *14*, 2444−2450.
(15) Pashley, R. M. *J. Colloid Interface Sci.* **1981**, *80*, 153.
(16) Van der Voort, P.; Gillis-D'Hamers, I.; Vansant, E. F. *J. Chem. Soc., Faraday Trans.* **1990**, *86*, 3751−5.
(17) Manne, S.; Gaub, H. E. *Science* **1995**, *270*, 1480−2.
(18) Liu, J.-F.; Ducker, W. A. *J. Phys. Chem. B* **1999**, *103*, 8558−8567.
(19) Subramanian, V.; Ducker, W. A. *Langmuir*, submitted for publication.

Table 1. Refractive Index Increments of C_{16}TAB, C_{16}TAC, and $C_{16}TA^+$. Theoretical Calculations and Measured Values

			V		dn/dc_{calcd}		dn/dc_{measd}	
species	A, mL/mol	A/M, mL/g	mL/mol	mL/g	mL/g	mL/mol	mL/g	mL/mol
C_{16}TAB	105.1	0.288	324.4	0.89	0.20	72.7	0.143	52.0
C_{16}TAC	102.2	0.319	323.2	1.01	0.21	67.7	0.145	46.3
$C_{16}TA^+$	96.0	0.337	307.7	1.08	0.22	61.7		

of the silica surfaces and found it to be 1.7 nm over a (10 μm)^2 region and 0.3 nm over a (300 nm)^2 region. All experiments were at 25 °C and natural pH (~5.6).

Reflectometry. We measured surfactant adsorption using optical reflectometry. A major advantage of this technique is that it is not necessary to dry adsorbed layers for analysis and it therefore directly complements in situ AFM imaging studies. It provides an in situ measurement of adsorption kinetics with better than 1 s time resolution. Details of the technique, including its capabilities and limitations, are described elsewhere.[12,13,20,21] Briefly, optical reflectometry is based on the change in the interfacial refractive index profile caused by adsorption. When the interface is illuminated by a parallel (p-) polarized laser beam at an angle of incidence close to the Brewster angle, θ_B, the change in the interfacial refractive index profile produces a significant change in reflectivity, R_p. For the layer thicknesses produced by surfactant adsorption, the thickness and refractive index of the adsorbed layer cannot be reliably decoupled in the reflectivity analysis. Nevertheless, the surfactant surface excess concentration is reliably calculated from the optical average thickness, d, and the optical average refractive index, n, of the adsorbed layer via[21,22]

$$\Gamma = \frac{d(n - n_0)}{dn/dc} \tag{1}$$

where n_0 is the refractive index of the bulk solution and dn/dc is the refractive index increment of the surfactant. We measured the latter by differential refractometry.

To measure adsorption kinetics, we continuously measured the reflectivity at θ_B and used the approximation (good to within 2% for the 20-nm oxide layers typical of surfaces used in this study[21])

$$\Gamma(t) = A\{R_p^{1/2}(\theta_B,t) - R_p^{1/2}(\theta_B,0)\} \tag{2}$$

The proportionality constant, A, depends only on the oxide layer refractive index and thickness and is readily generated from a homogeneous two-layer optical model.[13,21]

We measured the oxide layer thickness prior to adsorption in each experiment by scanning angle reflectometry: measuring $R_p(\theta)$ over a range of angles centered on θ_B and then regressing that reflectivity profile against the optical model.[12] The refractive index of bulk silicon is $3.882 + 0.019i$ at the helium−neon laser wavelength of 632.8 nm. For the oxide layer, we use the refractive index of silica, $n_{oxide} = 1.46$.

We used the instrument described in Pagac et al.[13] with a rectangular slit flow cell except that the peristaltic pump we previously used to flow solution over the surface has been replaced by a glass syringe and syringe pump. All tubing was Teflon. The wall shear rate in all experiments was a constant 3.67 s^{-1}. Temperature was controlled at 25 °C by circulating constant temperature water from a bath through the flow cell housing.

Microscopy. We used a Nanoscope III AFM (Digital Instruments) to image adsorbed surfactant layers using the "soft contact" mode described previously,[7,23] where the adsorbed layer is imaged via repulsive forces which maintain the tip at a finite separation from the surface. The silicon nitride cantilevers, from Olympus, had sharpened tips with a radius of less than 20 nm and a spring constant of 0.09 N m^{-1}. The ultralevers were irradiated (approximately 9 mW/cm^2 at 253.7-nm wavelength) for 45 min in a laminar flow cabinet before use. The scanner was calibrated in lateral dimensions by using a 1-μm grid and in the z direction by using a 180-nm-deep etch pit standard. All images shown are deflection images and with scan rates of 10 Hz with integral and proportional gains between 1 and 3. Deflection images are presented rather than height images because the measured height changes are very small (approximately 0.2 nm), which yields low quality height images.

To begin each AFM experiment, we introduced Milli-Q water into the liquid cell and imaged the silica surface in contact mode to assess surface cleanliness. Following this, we injected the surfactant solution, passing at least 50× the volume of the cell over the surface. The solutions were usually allowed to adsorb for 30 min before imaging, although no difference was found in the structures when imaged at times as short as 5 min after injection.

Results and Discussion

Surfactant Characterization. We measured the critical micelle concentration of C_{16}TAB and C_{16}TAC both with and without 10 mM salt using surface tension, conductivity, and fluorescence spectroscopy. For the fluorescence experiments, solutions contained 0.5 μM pyrene and the cmc was indicated by a sharp decrease in the I_1/I_3 ratio.[24] No minimum in surface tension was observed near the cmc, indicating the absence of significant surface active impurities. Conductivity was used only on solutions without added electrolyte. Surface tension, conductivity, and fluorescence spectroscopy gave consistent values for the critical micelle concentrations. We found cmc values of 0.94 ± 0.08 mM and 1.45 ± 0.12 mM without added salt for C_{16}TAB and C_{16}TAC, respectively. In the presence of 10 mM salt, the cmc values were 0.12 ± 0.02 mM for C_{16}TAB in KBr and 0.25 ± 0.02 mM for C_{16}TAC in KCl.

Refractive Index Increments. Artifacts in optical measurements of the surface excess concentration may arise when the refractive index increment of adsorbed surfactant differs from the value measured in solution. This could occur, for example, if dn/dc were to depend on the degree of counterion binding and if this in turn were to vary between the micelles in solution and the adsorbed layer.

Using a Brice-Phoenix differential refractometer, we measured the refractive index increment for micellar C_{16}TAB and C_{16}TAC solutions. Because the refractive indices of dilute (below cmc) solutions are too close to that of pure water, we cannot measure the refractive index increment of the fully dissociated monomeric surfactant. The measured refractive index increments are shown in Table 1 in both molar and mass units.

We also calculated the refractive index increments of the surfactants using an equation derived from the Lorentz−Lorenz relation for the refractive index n of a binary mixture:

(20) Charron, J. R.; Tilton, R. D. *J. Phys. Chem.* **1996**, *100*, 3179−89.
(21) Tilton, R. D. Scanning Angle Reflectometry and Its Application to Polymer Adsorption and Coadsorption with Surfactants. In *Colloid−Polymer Interactions: From Fundamentals to Practice*; Farinato, R. S., Dubin, P. L., Eds.; John Wiley & Sons: New York, 1999; pp 331−363.
(22) de Feijter, J. A.; Benjamins, J.; Veer, F. A. *Biopolymers* **1978**, *17*, 1759−1772.
(23) Fleming, B. D.; Wanless, E. J. *Microscopy and Microanalysis*; in press.
(24) Kim, J.-H.; Domach, M. M.; Tilton, R. D. *Colloids Surf. A: Physiochem. Eng. Asp.* **1999**, *150*, 55−68.

$$c = \frac{n^2 - n_w^2}{(A/M)(n^2 + 2)(n_W^2 + 2) - V(n_W^2 - 1)(n^2 + 2)} \quad (3)$$

where A/M is ratio of the molar refractivity to the molecular weight of the substance, V is the partial specific volume of the substance, c is the concentration (g/mL) of the substance, and n_w is the refractive index of the solvent, water in this case.[25] We calculated A/M by the bond additivity method.[26] Values for A/M are shown in Table 1 for C_{16}TAB, C_{16}TAC, and $C_{16}TA^+$. Gianni and Lepori used a group additivity method to calculate the partial *molar* volume for many ionic organic solutes in aqueous solution. Their value for C_{16}TAB is shown in Table 1.[27] They report that this value is within 1% of the experimentally determined value. Table 1 also shows partial molar volumes for C_{16}TAC and $C_{16}TA^+$ calculated by using the same additivity methods. The partial *specific* volumes, used in eq 3, are also shown there. The refractive index increments of C_{16}TAB, C_{16}TAC, and $C_{16}TA^+$ thus calculated via eq 3 are shown in Table 1.

The calculated values are approximately 30% larger than the measured values. The discrepancy may occur because of a specific volume difference between monomeric and micellized surfactant that is not taken into account in the calculation. Since the packing of adsorbed surfactants will more closely resemble micelles than freely dissolved monomers, we chose to use the refractive index increments measured for micellar solutions to analyze reflectometry data.

Since we are interested in the effect of the counterion on the adsorbed amount, we need to investigate the optical effect of the counterion. Table 1 shows that changing the counterion from Br^- to Cl^- will change the refractive index increment by at most 12% (based on measured values, or 7% based on calculated values). The largest error that could be expected due to unaccounted counterion binding effects would correspond to the difference in refractive index increments for $C_{16}TA^+$ (i.e., 0% counterion binding) and C_{16}TAB or C_{16}TAC with 100% counterion binding. Comparing the calculated dn/dc values, we conclude that this error is at most 18% for Br^- or 10% for Cl^-.

Surface Excess Concentrations. Figure 1 shows the adsorption isotherms for C_{16}TAB with and without 10 mM KBr. These resemble isotherms reported by others (in the absence of salt).[14] Above the cmc, the surface excess concentration is 3.0 ± 0.3 molecules/nm^2 (1.7 ± 0.2 mg/m^2) in the absence of KBr and 4.0 ± 0.3 molecules/nm^2 (2.3 ± 0.2 mg/m^2) in the presence of KBr. These correspond to mean molecular areas of 34 ± 4 and 25 ± 2 Å^2, respectively. Below the cmc, there is no statistical difference between the isotherms measured with or without added electrolyte, when the bulk surfactant concentration is normalized by the respective cmc.

The above results for C_{16}TAB differ from those previously reported from this group by Furst et al. and Pagac et al.[12,13] We reported an adsorption maximum in the isotherm at the cmc both with and without added electrolyte. We also reported biphasic desorption kinetics (fast initial desorption followed by slow desorption of a persistent fraction of the adsorbed layer that lasted for hours) for concentrations below the cmc, whereas desorption was complete under all conditions in the current study. Similar adsorption maxima have been ascribed

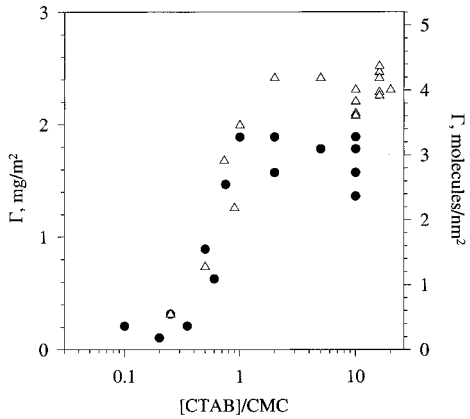

Figure 1. Adsorption isotherms for C_{16}TAB without added salt (closed circles) and with 10 mM KBr (open triangles). Concentration is normalized by the respective cmc value.

previously to surface-active impurities that can be removed by surfactant purification[28] and alternatively to the decrease in ionic surfactant monomer activity that occurs above the cmc.[29]

In the previous work we had tested for surfactant impurities by comparing adsorption results for C_{16}TAB used as received (>99% pure), for an especially pure (>99.9% pure) sample used as received, and for C_{16}TAB that we further purified by two fundamentally different methods. The adsorption results were identical for all experiments, and none of the surfactant solutions displayed a minimum in the surface tension. This led us to conclude that surfactant impurities were not the reason for the observed overshoot. We tested for impurities in the tubing system, water, and/or salt solutions by flowing surfactant-free water with and without added salt through our pumping system and over the surface for up to 24 h and observed no adsorption. Thus we ruled out water and salt as the source of the impurity and also believed (incorrectly) that surface-active impurities originating from the tubing/pumping system were not important. From this we concluded that if an impurity were indeed responsible for the overshoot, it had to be fundamentally different from the type of impurity usually blamed for adsorption maxima. It could not be intrinsically surface active but instead would have to adsorb only cooperatively with the surfactant. At the time, we favored an explanation that there were different adsorbed surfactant structures and/or altered counterion binding effects (and possible optical effects arising therefrom) near and above the cmc. These hypotheses prompted the current research.

We have now found, however, that the adsorption isotherm maximum was indeed the result of an impurity that adsorbed cooperatively with C_{16}TAB. This impurity came from the poly(vinyl chloride) (PVC) peristaltic pump tubing. The isotherm maximum and partial adsorption irreversibility disappeared when we replaced the peristaltic pump system by a syringe pump with a glass syringe. We believe that the impurity was sparingly soluble plasticizer from the PVC tubing that partitioned into the hydrophobic core of the adsorbed surfactant layer.

Figure 2 shows the adsorption isotherms for C_{16}TAC on silica with and without 10 mM KCl, with surfactant concentrations normalized by the respective cmc. The plateau values above the cmc are 1.7 ± 0.2 molecules/nm^2

(25) Cuypers, P. A. C., J. W.; Janssen, M. P.; Kop, J. M. M.; Hermens, W. Th.; Hemker, H. C. *J. Biol. Chem.* **1983**, *258*, 2426.
(26) Vogel, A. I.; Cresswell, W. T.; Jeffery, G. H.; Leicester, J. *J. Chem. Soc. Part I* **1952**, 514.
(27) Gianni, P.; Lepori, L. *J. Sol. Chem.* **1996**, *25*, 1−42.
(28) Arnebrant, T.; Backstrom, K.; Jonsson, B.; Nylander, T. *J. Colloid Interface Sci.* **1989**, *128*, 303−312.
(29) Evans, D. F.; Wennerström, H. *The Colloidal Domain*; Wiley-VCH: New York, 1994.

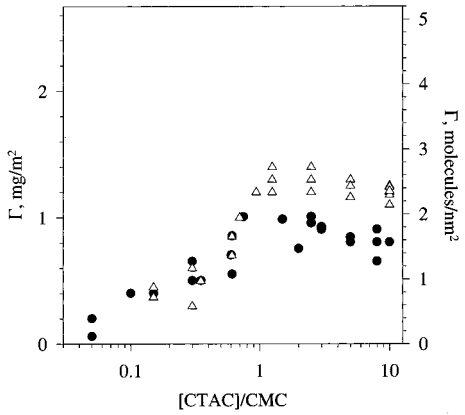

Figure 2. Adsorption isotherms for C_{16}TAC without added salt (closed circles) and with 10 mM KCl (open triangles). Concentration is normalized by the respective cmc values.

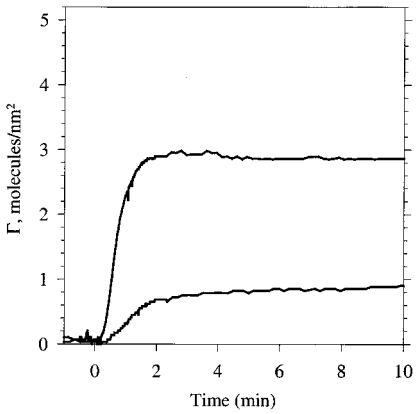

Figure 3. Adsorption kinetics for 7.5 mM C_{16}TAB (upper curve) and 0.5 mM C_{16}TAB (lower curve) in the absence of salt. The initial rate of adsorption is 2.0 and 0.3 mg/m^2/min for 7.5 and 0.5 mM C_{16}TAB, respectively.

(0.9 ± 0.1 mg/m^2) in the absence of KCl and 2.4 ± 0.2 molecules/nm^2 (1.3 ± 0.1 mg/m^2) in the presence of KCl. These correspond to mean molecular areas of 59 ± 7 Å^2 in the absence of KCl and 41 ± 3 Å^2 in the presence of KCl, as compared to 34 ± 4 and 25 ± 2 Å^2 for C_{16}TAB in the absence and presence of KBr, respectively. Therefore, above the cmc, there are approximately 60% fewer surfactants adsorbed for Cl^- vs Br^- counterions. This difference is much greater than can be explained by the optical effect of the counterion. We use these measured surface excess concentrations to interpret AFM images presented below.

Figure 3 shows adsorption kinetics for C_{16}TAB at 7.5 mM (8 × cmc) and 0.5 mM cmc (0.5 × cmc) with no added salt. Above the cmc, the plateau value of 3 molecules/nm^2 is reached within 2 min and remains stable for many hours (not shown). Upon rinsing, the layer completely desorbs within seconds (not shown). Both of these behaviors are the same as previously reported for micellar C_{16}TAB solutions,[13] since the abundant partitioning of impurity into micelles in solution evidently would have depleted it from the adsorbed layer.

At 0.5 × cmc, adsorption reached 80% of its plateau value after 2 min, much faster than previously reported.[13] Unlike the previous report, the adsorbed layer could also be removed completely at any time by rinsing with water. Compared to micellar solutions, the initial adsorption rate was slower for nonmicellar solutions, but we do not observe the extremely slow evolution to the final adsorbed amount (over many hours) that we previously reported.[13]

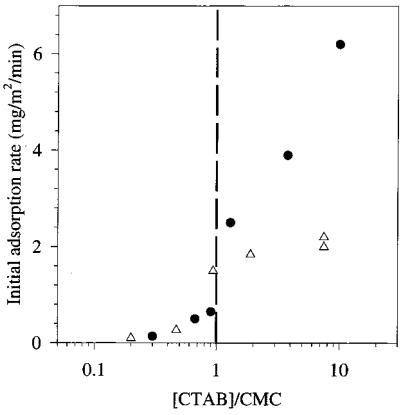

Figure 4. Initial rates of C_{16}TAB adsorption without added salt (closed circles) and with 10 mM KBr (open triangles). An abrupt change occurs at the cmc marked by the dashed line.

The initial adsorption rate is plotted as a function of C_{16}TAB concentration in Figure 4. There is a sharp increase in the initial adsorption rate at the cmc. This abrupt increase, also observed previously,[13] suggests that the adsorption mechanism changes at the cmc.[13] This could result from either altered mass transfer conditions or from surface effects. For example, one explanation is that micelles adsorb above the cmc whereas surfactant monomers adsorb below the cmc. Above the cmc, this could also be a mass transfer "source" effect: micelles may serve as a source of monomeric surfactants to rapidly replenish the surface sublayer as monomers adsorb.[30] Regardless of whether the change in initial adsorption rate at the cmc reflects altered mass transfer conditions or surface effects, it is clear that the initial rate behavior was not influenced by the impurity, as similar results were obtained both in this study and in the previous study. Since this impurity was not intrinsically surface active, the thermodynamic driving force for impurity partitioning would not have existed until after a surfactant layer with some hydrophobic domains had been established.

When normalized by the cmc, the initial adsorption rates are independent of salt concentration below the cmc. Above the cmc, the initial adsorption is faster in the absence of salt. This is likely because the addition of 10 mM KBr weakens the electrostatic attraction to the clean surface.

Figure 5 shows that the adsorbed amount of surfactant can be altered, reversibly, by changing the counterion. In this type of experiment, a solution containing 2 mM surfactant and 10 mM salt was continuously flowed over the surface, but the composition was periodically changed by switching between C_{16}TAB and C_{16}TAC and/or between KBr and KCl. In all cases, the added salt was responsible for supplying 83% of the total counterions in solution. In the case of C_{16}TAC with 10 mM KBr (5:1 ratio of Br^- to Cl^-), the adsorbed amount is the same as for C_{16}TAB with 10 mM KBr. However, when chloride is in excess of bromide, as when 10 mM KCl is added to a C_{16}TAB solution, the adsorbed amount falls between that observed for C_{16}TAC in KCl and C_{16}TAB in KBr. Therefore, when both types of counterion are present, there is a competition for binding to the surfactant micelles and adsorbed aggregates, and this competition in turn controls the surfactant surface concentration. These adsorption results are consistent with the bromide ion having a 5-fold greater binding affinity than chloride ion and therefore having a greater effect on the adsorbed amounts.

(30) Kabalnov, A.; Weers, J. *Langmuir* **1996**, *12*, 3442−3448.

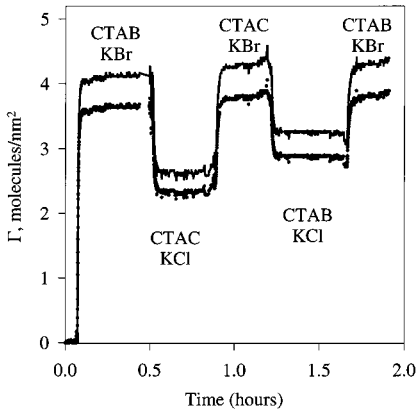

Figure 5. Response of adsorbed layer to discontinuous change in the type of counterion in solution. All solutions contain 2 mM $C_{16}TA^+ X^-$ in 10 mM KX where X is either Br^- or Cl^-. The composition is varied as follows: (1) C_{16}TAB in KBr; (2) C_{16}TAC in KCl; (3) C_{16}TAC in KBr; (4) C_{16}TAB in KCl; (5) C_{16}TAB in KBr. The upper curve is calculated by using the refractive index increment of C_{16}TAC and the lower curve by using the refractive index increment of C_{16}TAB.

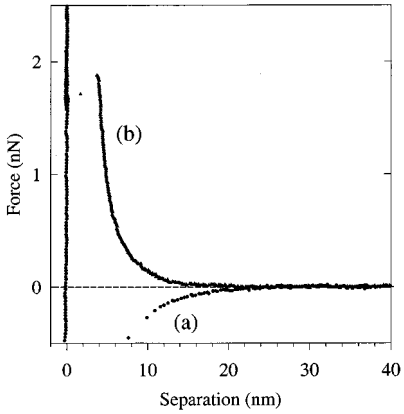

Figure 6. Force versus separation curves before (a) and after (b) $C_{16}TA^+$ adsorption on silica. After adsorption, the tip is pushed through the adsorbed layer from a distance of 3.5−4.0 nm. Force curves for C_{16}TAB and C_{16}TAC were similar.

Adsorbed Layer Structure. Figure 6 shows typical tip−surface force curves obtained on silica surfaces before and after adsorption of $C_{16}TA^+$. Before adsorption, the interaction between the silicon nitride tip and the negatively charged bare silica is purely attractive at natural pH in the absence of added salt. This is consistent with the force between silicon nitride tips and negatively charged mica surfaces reported by Senden and Drummond.[31] They found that, although there is a long range repulsive force above pH 9.5, the force is purely attractive at pH 5.6. They concluded from a study of silicon nitride vs mica and silicon nitride vs silicon nitride force measurements that the silicon nitride tips were net zero charged, or near to it, between pH 6 and 8.5.[32] Furthermore, Lin et al.[33] determined that the isoelectric point of fabricated silicon nitride AFM tips is 6.0 ± 0.4.

The force curve for the adsorbed surfactant layer is qualitatively consistent with previous AFM studies of adsorbed cationic surfactant layers.[9] On approach, the tip and the structure being imaged experience an electrostatic repulsion until a critical separation where the tip pushes though the adsorbed layer and falls into adhesive contact with the silica surface. This "push-through" distance provides a measure of the adsorbed layer thickness.[34] It was typically 3.5−4.0 nm for all experiments in this study (with and without 10 mM electrolyte and at all bulk concentrations of $C_{16}TA^+$). This is intermediate between one and two times the length of a $C_{16}TA^+$ surfactant (estimated as approximately 2.6 nm by adding the diameter of the headgroup to the length of the alkyl tail)[35] and is slightly less than the measured diameter of a $C_{16}TA^+$ micelle in solution (4.0−5.0 nm).[36] The 3.5−4.0 nm layer thickness reported here is consistent with the adsorbed layer thickness determined via neutron reflectivity for C_{16}TAB on quartz[11] and also consistent with the thickness of C_{16}TAB layers on opposing glass surfaces measured in a MASIF surface forces apparatus.[37] The magnitude of the measured push through distance coupled with the negligible charge on the tip suggest that there is no significant adsorption on the tip surface.

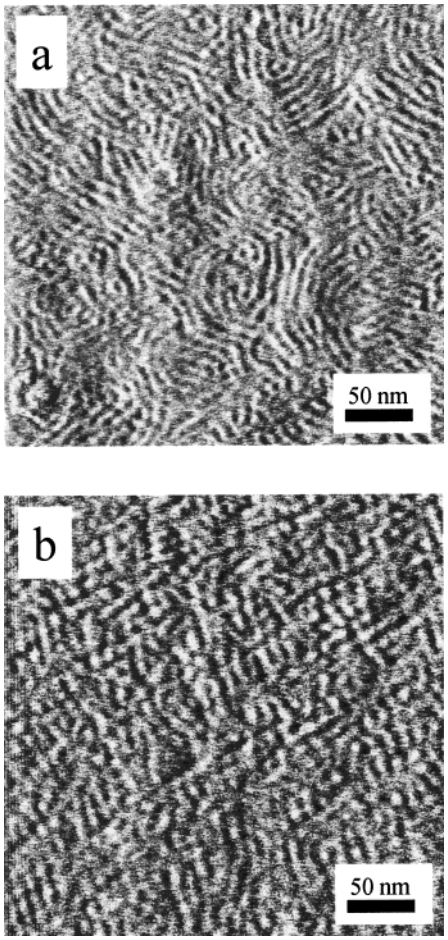

Figure 7. AFM images of adsorbed C_{16}TAB layers on silica. Both images are 300 nm × 300 nm and are obtained with forces on the repulsive part of the force curve. (a) "Wormlike" micelles observed at 10 × cmc. Similar structures are seen in the presence or absence of salt with a peak-to-peak distance of 10 nm in deionized water and 8 nm in the presence of 10 mM KBr. (b) Short rods and/or spheres coexist at 0.9 × cmc in both the absence and presence of 10 mM KBr.

C_{16}TAB. Figure 7a shows that C_{16}TAB adsorbed from

(31) Senden, T. J.; Drummond, C. J.; Kekicheff, P. *Langmuir* **1994**, *10*, 358−62.
(32) Drummond, C. J.; Senden, T. J. *Mater. Sci. Forum* **1995**, *189−190*, 107−13.
(33) Lin, X. Y.; Creuzet, F.; Arribart, H. *J. Phys. Chem.* **1993**, *97*, 7272−6.
(34) Wanless, E. J.; Ducker, W. A. *J. Phys. Chem.* **1996**, *100*, 3207−14.
(35) Tanford, C. *J. Phys. Chem.* **1972**, *76*, 3020−4.
(36) Magid, L. J. *J. Phys. Chem. B* **1998**, *102*, 4064−4074.
(37) Parker, J. L.; Yaminsky, V. V.; Claesson, P. M. *J. Phys. Chem.* **1993**, *97*, 7706−10.

a 10 × cmc solution with no added electrolyte forms wormlike micelles on silica. Similar structures were observed in all cases with and without 10 mM KBr at 10 × cmc. These wormlike structures (curved rodlike micelles) formed within 5 min of introducing the solution. Though wormlike micelles have been observed on mica surfaces,[8,9] this is the first time that wormlike C_{16}TAB micelles have been observed on silica. In a few cases, we observed a transition from wormlike micelles to a laterally homogeneous structure (presumably a bilayer), similar to that observed on mica.[8] It was very difficult to characterize this transition since it was not always seen in our experiments. In those experiments where it did occur, it did so after 8−12 h of adsorption. In most of the experiments it was not observed at all during approximately 1 day of adsorption.

Figure 7b is representative of C_{16}TAB layers adsorbed at 0.9 × cmc. Images were similar both in the absence and presence of KBr. There appears to be a coexistence of spheres and short rods. Since the isotherm in Figure 1 shows that the surface excess concentration attains a plateau just at the cmc, this may indicate that a structural transition occurs near the cmc. Further evidence is needed to prove this and is the subject of an ongoing investigation.

We cannot precisely resolve the contour of the aggregates since the size of the tip makes it impossible to measure the lateral size of an aggregate. Therefore, to quantitatively describe the layer structure at 10 × cmc, we measured the peak-to-peak distances instead of the apparent diameter of the wormlike micelles. The peak-to-peak distance equals the sum of the aggregate diameter plus the edge-to-edge separation and is independent of tip size. The peak-to-peak distances for the rodlike C_{16}-TAB aggregates are $b = 10 \pm 1$ nm in the absence of KBr and $b = 8 \pm 1$ nm in the presence of 10 mM KBr.

How do these images compare with the measured surface excess concentrations? Since AFM cannot resolve individual surfactant molecules, we make geometric arguments to estimate a surface excess concentration from the image. We assume, for the sake of the calculation, that the aggregates are linear in the long direction and that there is one rod per unit cell of width b (the calculation is independent of the length of the rodlike micelle). We calculate the surface excess concentration, Γ, as the number of surfactants in a unit micelle divided by the unit cell area:

$$\Gamma = \frac{N}{A_{\text{cell}}} = \frac{2\pi a/A_0}{b} \qquad (4)$$

where a is the radius of the rodlike micelle, A_0 is the mean molecular area per headgroup *in the micelle surface*, and b is the peak-to-peak distance. Although A_0 and a are unknown at the interface, we can estimate that $A_0 = 72$ Å^2 (equal to that reported for rodlike micelles in solution).[5] Using eq 4 and the experimental values for the surface excess concentration and peak-to-peak distance ($\Gamma = 3.0$ molecules/nm^2, $b = 10$ nm in 0 mM KBr; $\Gamma = 4.0$ molecules/nm^2, $b = 8$ nm in 10 mM KBr), we calculate the radius of the adsorbed rodlike micelle to be $a = 3.4$ and 3.7 nm in the absence and presence of KBr, respectively. In both cases, $2a < b$, indicating a finite edge-to-edge separation. Since the radius of the rodlike micelle in solution is 2.0−2.5 nm,[36] these calculations indicate that the adsorbed rodlike micelles are broader than rodlike micelles in solution. If instead one assumes that the radii are equal to 2.5 nm, the combined reflectometry and AFM results are consistent with surfactant packing at 52 Å^2 per headgroup in salt-free solution and 49 Å^2 per headgroup in 10 mM KBr. These are close to the 55 Å^2 packing observed for flat C_{16}TAB monolayers at the air/water interface.[12] In either case, the calculations suggest that adsorbed C_{16}TAB aggregates are somewhat different from rodlike micelles in solution. Since the estimate of the layer thickness based on the push-through distance, 3.5−4.0 nm, is less than $2a$, these wormlike aggregates are somewhat "flattened". The heterogeneity of structures observed at 0.9 × cmc makes them too complex to analyze in this way.

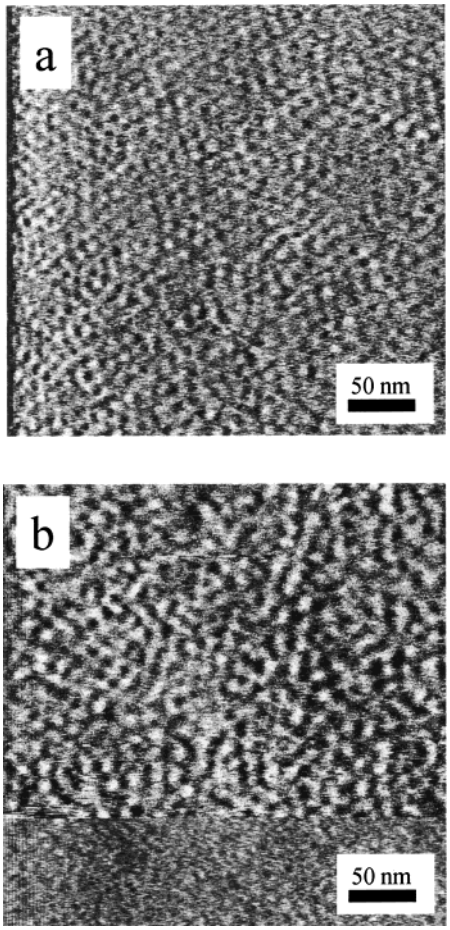

Figure 8. AFM images of adsorbed C_{16}TAC layers on silica. Both images are 300 nm × 300 nm and are obtained with forces on the repulsive part of the force curve. Adsorbed aggregates with circular projections are observed for both (a) 10 × cmc and (b) 0.9 × cmc. Peak-to-peak distances are 10 nm in (a) and 13 nm in (b). The bottom of the image in (b) shows where the tip was intentionally pushed through the layer to image the underlying silica surface in contact mode.

C_{16}TAC. Figure 8 shows adsorbed C_{16}TAC layers for 10 × cmc and 0.9 × cmc. Adsorbed C_{16}TAC layers consist of aggregates with circular projections under both conditions. To quantify the distance between the aggregates in these images, we performed a two-dimensional Fourier transform of the images and recorded the inverse reciprocal spacing for at least three images per experiment and for several experiments. The peak-to-peak distance between C_{16}TAC aggregates is 10 ± 2 nm at 10 × cmc and 13 ± 2 nm at 0.9 × cmc. The aggregates appear to be quite uniform in spacing and appearance across the surface. There is no statistically significant difference between the peak-to-peak distances in C_{16}TAC images recorded in the absence or presence of 10 mM KCl. Nevertheless, for concentrations above the cmc, reflectometry did indicate

a 0.7 molecule/nm^2 increase in the C_{16}TAC surface concentration with the addition of KCl (Figure 2).

Interesting conclusions arise when reconciling these images with the corresponding surface concentrations. We determined the number of aggregates per unit area, $\Gamma_{aggregate}$, by counting the number of adsorbed aggregates in areas ranging from 2400 to 1.2×10^5 nm^2. We sampled numerous areas from within one image, within different images from one experiment and within different images for different experiments conducted under identical conditions. At 10 × cmc, $\Gamma_{aggregate}$ is $(1.05 \pm 0.33) \times 10^{-2}$ aggregates/nm^2 in the absence of KCl and $(1.14 \pm 0.30) \times 10^{-2}$ aggregates/nm^2 in the presence of 10 mM KCl. Using the surface excess concentration measured by reflectometry ($\Gamma = 1.7 \pm 0.2$ and 2.4 ± 0.2 molecules/nm^2 in the absence and presence of KCl, respectively), we calculate average aggregation numbers of 161 ± 54 in the absence of KCl and 210 ± 58 in the presence of 10 mM KCl. At 0.9 × cmc, $\Gamma_{aggregate}$ is $(4.9 \pm 1.1) \times 10^{-3}$ aggregates/nm^2 and $\Gamma = 1.7$ molecules/nm^2 in both the absence and presence of salt. Thus the average aggregation number is 346 ± 89. Note that there are no geometric assumptions implicit in these calculations.

These adsorbed aggregates have significantly larger aggregation numbers than the typical 90−120 range of aggregation numbers reported for C_{16}TAC micelles in solution.[5] Even though the aggregation number of the adsorbed aggregates is larger than what would be found for micelles in solution, the estimate of the layer thickness based on the push-through distance, 3.5−4.0 nm, is less than the diameter of a spherical micelle in solution (4−5 nm). Therefore the aggregates may be considered "discoid" in shape.

Fan et al.[38] have previously shown, via fluorescence spectroscopy, that cationic surfactant aggregates adsorbed near the cmc on oppositely charged surfaces can be larger than micelles in solution. They observed aggregation numbers of 111−135 for C_{16}TAB on the surface of negatively charged alumina at concentrations very close to the cmc (compare to aggregation numbers of 75−95 typically reported for spherical C_{16}TAB micelles in solution[39]). They also found larger aggregation numbers of SDS on positively charged alumina (49−356).[38] We find it especially interesting that adsorbed aggregates formed below the cmc have significantly larger aggregation numbers than those formed above the cmc. As noted above with regard to the initial adsorption rate behavior (Figure 4), there is a possibility that micelles adsorb directly from the solution to the surface. Even if this were to occur, a separate process of interfacial self-assembly must be occurring in order to produce adsorbed aggregates whose aggregation numbers are larger than those of micelles in solution.

Comparing C_{16}TAC and C_{16}TAB, it is evident that the counterion can select whether rods or "discoids" form on the surface. Just as occurs in solution, bromide is better able than chloride to stabilize rodlike micelles on the surface because of its higher binding affinity and deeper penetration into the micelle. This structural change is very significant; it accounts for a 66% decrease in the adsorbed amount for C_{16}TAC relative to C_{16}TAB.

Recalling the discussion of the differences between silica and mica, it is appropriate here to compare the $C_{16}TA^+$ adsorption on these two surfaces. Above the cmc, cylindrical C_{16}TAB micelles form on the surface of both silica and mica. On mica the peak-to-peak distance is 7 nm for C_{16}TAB at 2 × cmc with no salt present,[9] whereas we found the peak-to-peak distance to be 10 ± 1 nm without salt and 8 ± 1 nm with 10 mM KBr at 10 × cmc. Since the surface excess concentration was constant for C_{16}TAB on silica above the cmc, we assume that the peak-to-peak distance would be the same at 2 × cmc as at 10 × cmc. The difference between silica and mica may be explained by either variation in actual micelle size (more flattened micelle on silica) or in micelle edge-to-edge separation, since the peak-to-peak distances include both lengths. However, the possibility for more extensive ion pairing with the mica surface should be expected to reduce the effective headgroup area and thus lead to increased aggregate flattening on mica. As this appears not to be the case, this suggests that there is a larger edge-to-edge aggregate spacing on silica.

The difference in charge between mica and silica also affects the "linearity" of the wormlike micelles. On silica, the structures are much more curved in the axial direction (less linear) than those found on mica with no added salt. However, the structures on mica do become less linear when more KBr is added, due to a competition between the K^+ ions and the $C_{16}TA^+$ for the negative lattice sites.[9] Therefore, decreasing the availability of negative surface sites, either by adsorbing more cations to mica or by using silica as the surface instead of mica, causes the rodlike micelles to become less linear.

A structural transition on the surface depends on both the binding affinity of the surfactant counterion and the charge of the underlying substrate. On mica, both C_{16}TAB and C_{16}TAC form rodlike micelles (low aggregate curvature) with no added salt.[8] On silica, we find that C_{16}TAC forms "discoids" (higher aggregate curvature).

As pointed out previously[9] the negatively charged surface sites act as "counterions" to the surfactant aggregates. Mica, with its higher density of ionizable sites, is better able to stabilize lower aggregate curvature. It is interesting to note that on mica C_{12}TAC forms spheres whereas C_{12}TAB remains rodlike.[10] Thus the structure of adsorbed surfactant aggregates is controlled by all the parameters that control structure in solution (counterion binding, tail length, etc.) but with the extra effect of the underlying surface acting as a collection of "counterions".

Conclusions

We combined optical reflectometry and atomic force microscopy to study the effect of counterions on the evolution of adsorbed layers of $C_{16}TA^+$ on silica. Above the cmc, C_{16}TAB adsorbs as wormlike micelles that achieve more than a 60% greater surface excess concentration than the "discoids" formed by adsorbed C_{16}TAC. Reconciling the AFM images with the measured surface excess concentrations indicates that the wormlike C_{16}TAB aggregates either have somewhat larger radii or more intimate headgroup packing than wormlike C_{16}TAB micelles in solution. The adsorbed C_{16}TAC aggregates have circular cross-sections but larger aggregation numbers than spherical C_{16}TAC micelles in solution. Both observations point to interfacial self-assembly processes that occur after the surfactants arrive at the surface. For both C_{16}TAC and C_{16}TAB, adding 10 mM salt increases the adsorbed amount and, in the case of C_{16}TAB, allows closer packing of adjacent wormlike micelles on the surface.

The adsorption kinetics suggest a change in the $C_{16}TA^+$ adsorption mechanism near the cmc. This is consistent with AFM images that show self-assembled structures at 0.9 × cmc that are different from those observed above

(38) Fan, A.; Somasundaran, P.; Turro, N. J. *Langmuir* **1997**, *13*, 506−510.

(39) Lianos, P.; Zana, R. *J. Colloid Interface Sci.* **1981**, *84*, 100−107.

the cmc. Whereas C_{16}TAB adsorbed above the cmc takes the form of rodlike aggregates, layers of C_{16}TAB adsorbed at 0.9 × cmc appear to contain a combination of discoids (possibly very short rods) and rods. C_{16}TAC forms discoidal aggregates at both 0.9 × cmc and 10 × cmc, but the calculated aggregation number is much higher below the cmc than above the cmc.

Compared to mica, the lower charge density of silica results in the following differences: an increase in the spacing between wormlike C_{16}TAB aggregates, greater axial curvature of adsorbed C_{16}TAB aggregates, and a greater sensitivity of the structure of $C_{16}TA^+$ aggregates to the counterion binding affinity.

Finally, we have now shown that overshoots in previously reported adsorption isotherms for C_{16}TAB on silica were caused by an impurity that leached out of PVC peristaltic pump tubing. Although the impurity was not intrinsically surface active on silica, it did partition into a layer of adsorbed surfactant. The impurity only affected the reversibility and extent of adsorption below the cmc. It did not affect the initial adsorption rates, nor did it affect the reversibility or extent of adsorption above the cmc.

Acknowledgment. This material is based on work supported by the National Science Foundation under Grant CTS-9623849, the Center for Multiphase Processes at the University of Newcastle, and a National Science Foundation Doctoral Fellowship for S.B.V. We thank the Carnegie Mellon University Department of Chemical Engineering for partial travel support for S.B.V.

LA9910935